

# 3D Quantitative Microwave Imaging with a Regularized Gauss-Newton Method for Breast Cancer Detection

Jürgen De Zaeytijd<sup>1</sup> and Ann Franchois<sup>2</sup>

<sup>1</sup> Department of Information Technology (INTEC), Ghent University,  
Sint-Pietersnieuwstraat 41, B-9000 Gent, Belgium  
[jurgen.dezaeytijd@intec.ugent.be](mailto:jurgen.dezaeytijd@intec.ugent.be)

<sup>2</sup> Department of Information Technology (INTEC - IMEC), Ghent University,  
Sint-Pietersnieuwstraat 41, B-9000 Gent, Belgium  
[ann.franchois@intec.ugent.be](mailto:ann.franchois@intec.ugent.be)

**Abstract:** The application of a three-dimensional Vectorial Quantitative Microwave Tomography (VQMT) algorithm to the challenging problem of 3D complex permittivity reconstruction in biological tissues is investigated. In particular, a simulation study on breast cancer imaging is conducted, using dipole excitations in various polarizations and positions in front of the breast at a single frequency. The algorithm is an improved version of the regularized Gauss-Newton imaging method recently presented by the authors. More specifically the application of a subspace preconditioned LSQR algorithm to the Gauss-Newton update systems improves the computational efficiency of the method and the incorporation of constraints and patient specific discretization of the permittivity extend its flexibility and application range.

**Keywords:** Microwave tomography, Complex permittivity, Non-linear inverse scattering, Breast cancer detection and 3D reconstruction.

## 1. Introduction

It has been pointed out that the electromagnetic properties (permittivity and conductivity) in the microwave frequency range (300 MHz - 30 GHz) differentiate between tissue types and various physiological and pathological parameters. This suggests quantitative 3D microwave imaging as a moderately-cost, non-invasive and non-ionizing supplemental technology to existing modalities in medical imaging. Such may be particularly the case with microwave breast cancer imaging, for the breast is an accessible volume to microwaves and the contrast in dielectric properties between malignant and normal tissues at these frequencies appears to be large.

Several types of 3D microwave imaging algorithms have been proposed for medical imaging in general and for breast cancer detection in particular. Vectorial Quantitative Microwave Tomography [1,2] (VQMT) attempts to determine the permittivity and conductivity values in each voxel of the investigation domain, by solving the 3D non-linear vectorial inverse scattering equations. Confocal Microwave Imaging (CMI) [3] on the other hand uses an ultrawideband Synthetic Aperture

Radar technique to reconstruct a qualitative image of the tumor and requires detailed information on the frequency dependent mean dielectric properties of the breast tissues. Reconstructions with the multi-view VQMT proposed in the present paper can be done at one single frequency and thanks to its quantitative character the introduction of accurate a priori information on tissue properties is not required.

A 3D regularized Gauss-Newton VQMT algorithm was presented by the authors in [2]. In this paper we propose several improvements to this algorithm: (i) A further reduction of the computational effort by a computationally more efficient and stable solution of the Gauss-Newton permittivity updates by means of a preconditioned LSQR algorithm [4]. (ii) The possibility to introduce *a priori* information in a flexible way, by allowing the inversion for pre-defined aggregates of permittivity voxels, instead of for each voxel independently. (iii) The proposal of a new, constrained line-search path in the Gauss-Newton optimization, which incorporates in an elegant manner *a priori* knowledge concerning lower and upper bounds on the permittivity.

## 2. Problem Formulation

Consider a 3D complex permittivity profile  $\epsilon(\mathbf{r}, \omega)$  in an investigation domain  $\mathcal{D}$  (Fig. 1(a)). Outside  $\mathcal{D}$ , the permittivity is homogeneous and equal to  $\epsilon_b$ . In the following, the dependency of the permittivity on  $\omega$ , the angular frequency, as well as the  $e^{j\omega t}$  dependency of the electric fields are implicitly assumed.

In order to reconstruct  $\epsilon(\mathbf{r})$  (solving the *inverse scattering problem*), scattering data are collected by successively illuminating the object with a number  $N^I$  of different known time-harmonic incident fields  $\mathbf{E}_i^{\text{inc}}$ , with  $i = 1, \dots, N^I$ , and by measuring for each illumination some components of the resulting scattered electric field vector  $\mathbf{E}_i^{\text{scat}}$  in a number of receiver points. The scattered field for an illumination  $\mathbf{E}_i^{\text{inc}}$  and a permittivity function  $\epsilon$  can also be calculated by solving the vector contrast-source integral equation [2]. Let  $L(\epsilon)$  be the linear integral operator that links the scattered field in the observation point  $\mathbf{r}$  to the total electric field  $\mathbf{E}_i$  in  $\mathcal{D}$ ,

$$\mathbf{E}_i^{\text{scat}}(\mathbf{r}) = [L(\epsilon)\mathbf{E}_i](\mathbf{r}), \quad (1)$$

then the vector contrast-source integral equation or *domain equation* is given by

$$\mathbf{E}_i^{\text{inc}}(\mathbf{r}) = \mathbf{E}_i(\mathbf{r}) - [L(\epsilon)\mathbf{E}_i](\mathbf{r}), \quad \forall \mathbf{r} \in \mathcal{D}. \quad (2)$$

Simulation of the scattered field, or solving the *forward scattering problem*, thus involves the solution of (2) for  $\mathbf{E}_i(\mathbf{r})$  in  $\mathcal{D}$  and the evaluation of the *observation equation* (1) in the observation points.

For the numerical inversion, the permittivity is parameterized on a uniform grid  $\mathcal{D}^\epsilon$  with cell size  $\Delta_\epsilon$  and with  $N^\epsilon = F \times G \times H$  identical cubic cells in the  $x$ -,  $y$ - and  $z$ -directions, respectively (Fig. 1(b)). The permittivity is approximated with a piecewise constant function

$$\epsilon(\mathbf{r}) \approx \sum_{n=1}^N \epsilon_n \epsilon_b \Phi_n(\mathbf{r}), \quad (3)$$

where the expansion functions  $\Phi_n$  have non-overlapping supports — consisting of one or more grid cells, hence  $N \leq N^\epsilon$  — that cover the complete grid  $\mathcal{D}^\epsilon$  and they assume the value 1 inside their support and are zero elsewhere. Some of the coefficients  $\epsilon_n$  may be known *a priori* and the other,

unknown, coefficients  $\epsilon_\nu$ , with  $\{\nu\}$  a subset of  $\{n\}$ , constitute the optimization variables. The coefficients  $\epsilon_\nu$  are collected in the  $N^{\text{opt}}$ - dimensional vector

$$\boldsymbol{\epsilon}^{\text{opt}} = [\epsilon_\nu], \quad (4)$$

with  $N^{\text{opt}} \leq N$ .

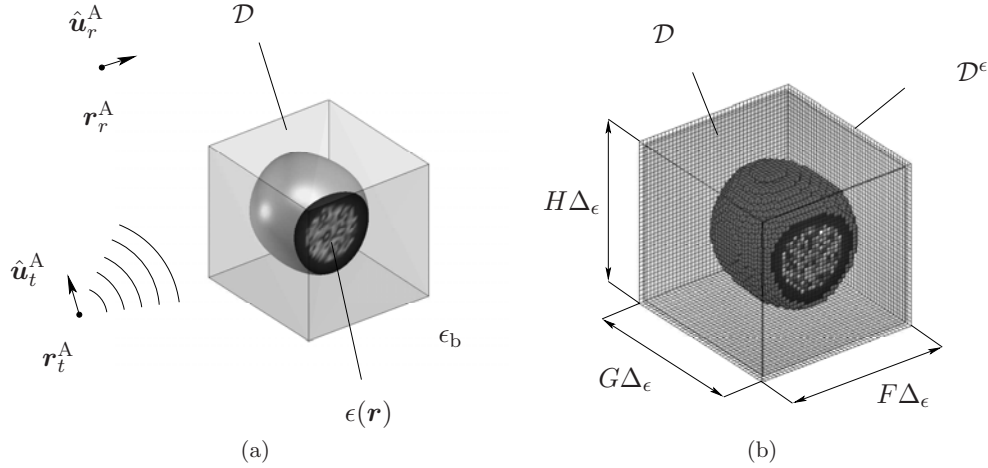


Fig. 1. The 3D scattering configuration: (a) general notations and definitions and definitions for the permittivity grid  $\mathcal{D}^\epsilon$  and (b) the piecewise constant approximation for the permittivity function.

### 3. VQMT Reconstruction Algorithm

The solution  $\boldsymbol{\epsilon}_{\text{sol}}^{\text{opt}}$  of the inverse scattering problem (1),(2) is redefined as the minimizer of the following regularized least squares cost function

$$\mathcal{F}(\boldsymbol{\epsilon}^{\text{opt}}) = \mathcal{F}^{LS}(\boldsymbol{\epsilon}^{\text{opt}}) [1 + \alpha \mathcal{F}^R(\boldsymbol{\epsilon}^{\text{opt}})], \quad (5)$$

where  $\mathcal{F}^{LS}$  is the least squares data error,  $\mathcal{F}^R$  is a smoothing function and  $\alpha$  a regularization parameter. The least squares data error is defined as

$$\mathcal{F}^{LS}(\boldsymbol{\epsilon}^{\text{opt}}) = \frac{1}{\mathcal{N}^{LS}} \|e^{\text{scat}}(\boldsymbol{\epsilon}^{\text{opt}}) - e^{\text{meas}}\|^2, \quad (6)$$

where  $e^{\text{meas}}$  and  $e^{\text{scat}}(\boldsymbol{\epsilon}^{\text{opt}})$  are  $N^{\text{D}}$ -dimensional vectors that contain, respectively, the measured scattered field data for all used combinations of transmitters and receivers, and the corresponding scattered field components computed for a given optimization vector  $\boldsymbol{\epsilon}^{\text{opt}}$ .  $\mathcal{N}^{LS} = \|e^{\text{meas}}\|^2$  is a normalization constant.

The minimization is done by performing successive line searches along descent paths. In iteration  $k$ , the line search path starts along the direction  $\mathbf{s}_k^{\text{opt}}$ , which is solution to the Gauss-Newton system

$$(\mathbf{J}_k^H \mathbf{J}_k + \lambda_k^2 \boldsymbol{\Sigma}) \mathbf{s}_k^{\text{opt}} = -(\mathbf{J}_k^H [e_k^{\text{scat}} - e^{\text{meas}}] + \lambda_k^2 \boldsymbol{\Omega}_k^*), \quad (7)$$

where  $\cdot^H$  stands for conjugate  $\cdot^*$  transpose  $\cdot^T$ , where

$$\lambda_k^2 = \frac{\alpha \mathcal{N}^{LS} \mathcal{F}_k^{LS}}{1 + \alpha \mathcal{F}_k^R}, \quad (8)$$

and where the subscript  $k$  indicates quantities evaluated in  $\epsilon_k^{\text{opt}}$ . Furthermore,  $\mathbf{J}$  is the  $N^D \times N^{\text{opt}}$  Jacobian matrix,  $J_{d\nu} = \partial e_d^{\text{scat}} / \partial \epsilon_\nu$ ;  $\boldsymbol{\Omega}$  is an  $N^{\text{opt}}$ -dimensional vector that contains the derivatives of the regularizing function,  $\Omega_\nu = \partial \mathcal{F}^R / \partial \epsilon_\nu$ ;  $\boldsymbol{\Sigma}$  is a real, constant matrix,  $\Sigma_{\nu\nu} = \partial^2 \mathcal{F}^R / \partial \epsilon_\nu \partial (\epsilon_\nu)^*$ .

In order to improve the convergence of the optimization technique, it is recommended to include *a priori* knowledge concerning the expected upper and lower bounds on the complex permittivity in the breast, by means of constraints. Such constraints also avoid the complex permittivity values from becoming non-physical or too high to handle with the chosen discretization  $\Delta_\epsilon^F$ , in which case the conditioning of the forward problem generally is very bad. We implemented the constraints by using smooth line search paths that start along the update directions (7), but bend away from this direction in the neighborhood of the constraints [5]. This allows for the introduction of constraints with a minimum of changes in the unconstrained optimization code: only the line search has to be modified.

Since their condition number can become unpleasantly high in the course of the iterations, the solution of the systems (7) is done with the subspace preconditioned LSQR algorithm of Jacobsen, et al. [4]. The key idea is a splitting of the solution space in two subspaces, one of which with a small dimension and one with a larger dimension. The small subspace can be regarded as a coarse grid approximation to the inverse scattering problem and the part of the solution vector in this subspace contributes most to the left hand side of (7). The projection of the update system on the larger subspace is better conditioned than the original problem and is solved iteratively, after which the contribution in the smaller subspace is obtained through direct solution of a small system that inherits the ill-conditioning of the original system.

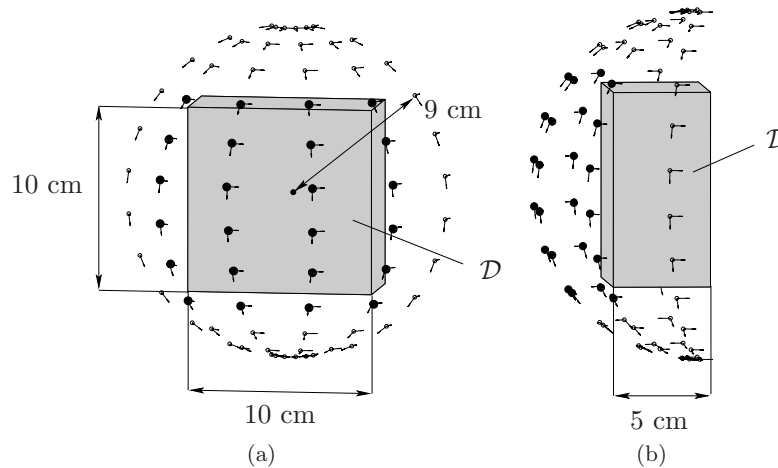


Fig. 2. The antenna configuration that is used in the numerical examples from two different view angles. The arrows visualize the orientation of the elementary dipoles and the large black dots indicate antennas that are both transmitter and receiver. The shaded cuboid is the investigation domain  $\mathcal{D}$ .

#### 4. Numerical Examples

We present reconstructions for two malignant breast numerical phantoms, one without and one with a skin layer, surrounded with a matching medium with permittivity  $\epsilon_b = 10\epsilon_0$ . The tumor has a size of 2 cm and relative complex permittivity  $\epsilon_{\text{tumor}}/\epsilon_0 = 49.93 - j14.43$ . It is embedded in a homogeneous, averaged breast tissue with permittivity  $\epsilon_{\text{breast}}/\epsilon_0 = 9.99 - j2.82$ . The breast is modelled as a hemisphere with radius 5 cm and for the phantom with skin is covered with a 2.5 mm skin layer with permittivity  $\epsilon_{\text{skin}}/\epsilon_0 = 40.94 - j16.17$ . The operating frequency is 1 GHz, yielding a wavelength of  $\lambda_b = 9.5$  cm in the matching medium. The antenna configuration is depicted in Fig. 2. The investigation domain  $\mathcal{D}$ , with dimensions 5 cm  $\times$  10 cm  $\times$  10 cm, is also indicated. The data are simulated by solving the vector contrast-source integral equation and Gaussian noise is added such that  $\text{SNR} = 30$  dB.

The reconstruction of the breast without skin is performed on a grid with cell size 0.5 cm. The result after 6 Gauss-Newton updates is shown in Fig. 3, where it can be seen that the permittivity value of the tumor is not correct, but the tumor is clearly visible at the right location and with a higher permittivity and conductivity than the surrounding breast tissue. Note that, considering the limited aperture data and the small dimensions of the tumor with respect to the matching medium wavelength, this result is quite satisfactory.

For the phantom with skin, the permittivity grid has a smaller cell size of 0.25 cm to allow modelling of the skin layer. To retain an over-determined system, to use as much a priori information as possible on this challenging reconstruction and to illustrate the possibilities of the improved algorithm, we assume the skin layer known and only optimize for permittivity cells inside the inner skin contour. Moreover, we optimize for aggregates of permittivity cells that are cubes (or portions of cubes) with side 0.5 cm. Finally, we use the constraints  $0.8 \leq \Re(\epsilon(\mathbf{r})/\epsilon_b) \leq 5$  and  $-0.1 \leq \Im(\epsilon(\mathbf{r})/\epsilon_b) \leq 0.1$  on the permittivity. The result after 5 Gauss-Newton updates is shown in Fig. 4. Again, the tumor is clearly visible, at the right location and with a higher permittivity and conductivity than the surrounding breast tissue, but these values are not entirely reconstructed.

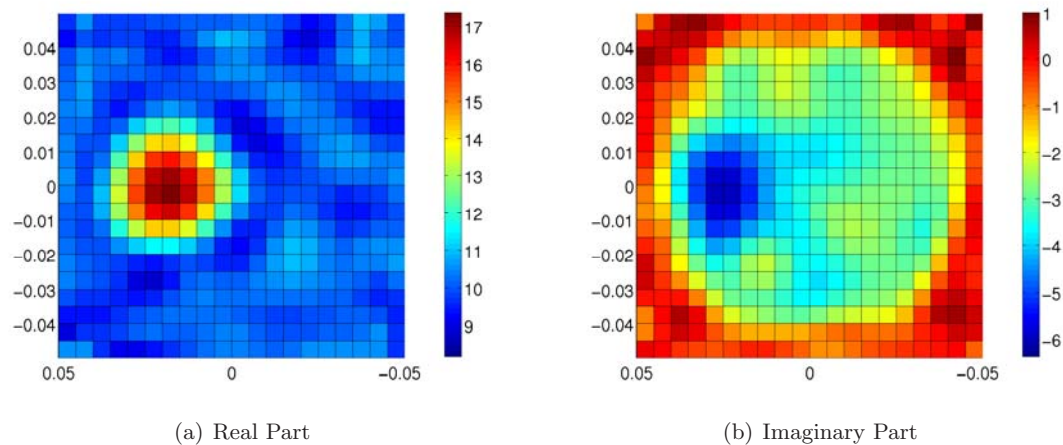


Fig. 3. The reconstructed complex permittivity in a vertical slice through the investigation domain and the center of the tumor for the phantom without skin.

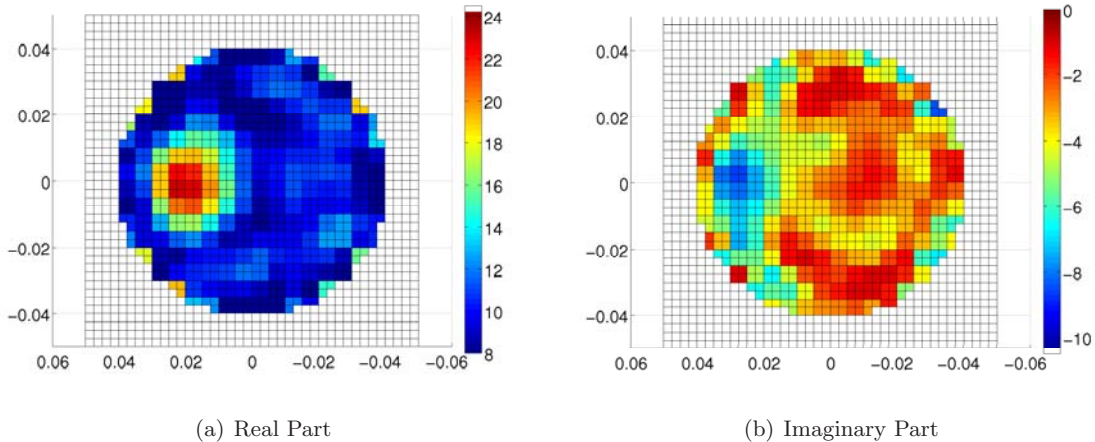


Fig. 4. The reconstructed complex permittivity in a vertical slice through the investigation domain and the center of the tumor for the phantom with skin. The permittivity cells that are not optimized for are coloured white.

## 5. Conclusions

We have presented an efficient three-dimensional Vectorial Quantitative Microwave Tomography reconstruction technique, which is based on a regularized Gauss-Newton optimization scheme and which is able to reconstruct the spatial complex permittivity distribution in biological objects at one single frequency, thereby avoiding difficulties with the dispersive nature of body tissues. In particular, numerical experiments have shown that the method can be applied to the challenging problem of breast tumor detection. This is largely made possible by the increased ability of the method to incorporate *a priori* information in the inversion scheme.

## References

- [1] A. Abubakar, P.M. van den Berg, J.J. Mallorqui, "Imaging of Biomedical Data Using a Multiplicative Regularized Contrast Source Inversion Method", *IEEE Trans. Microw. Theory Tech.*, Vol. 50, No. 7, pp. 1761-1770, 2002.
- [2] J. De Zaeytijd, A. Franchois, C. Eyraud, J.M. Geffrin, "Full-wave three-dimensional microwave imaging with a regularized Gauss-Newton method – theory and experiment", *IEEE Trans. Antennas Propagat.*, Vol. 55, No. 11, pp. 3279 - 3292, 2007.
- [3] E.C. Fear, X. Li, S.C. Hagness, M.A. Stuchly, "Confocal microwave imaging for breast tumor detection: Localization in three dimensions", *IEEE Trans. Biomed. Eng.*, Vol. 49, pp. 812-822, August, 2002.
- [4] M. Jacobsen, P.C. Hansen, M.A. Saunders, "Subspace preconditioned LSQR for discrete ill-posed problems", *BIT Numerical Mathematics*, Vol. 43, No. 5, pp. 975-989, 2003.
- [5] J. De Zaeytijd, A. Franchois, "Three-dimensional Vectorial Quantitative Microwave Tomography: Breast Imaging with a LSQR Preconditioned Regularized Gauss-Newton Method", submitted to *IEEE Trans. Medical Imag.*.